Journal of Molecular Graphics and Modelling 33 (2012) 12–18

Contents lists available at SciVerse ScienceDirect

Journal of Molecular Graphics and Modelling

journal homepage: www.elsevier.com/locate/JMGM

Binding of TNT to amplifying fluorescent polymers: An ab initio and molecular dynamics study

Mark A. Enlow*

Applied Research Associates, 421 Oak Avenue, Panama City, FL 32401, United states

ARTICLE INFO

Article history:
Received 15 March 2011
Received in revised form 1 September 2011
Accepted 3 September 2011
Available online 5 October 2011

Keywords:
Amplifying fluorescent polymer
Binding energy
Explosive detection
Molecular dynamics
Trinitrotoluene

ABSTRACT

Molecular modeling techniques were employed to study the interaction of trinitrotoluene with an amplifying fluorescent polymer used in explosive sensor devices. The pentiptycene moiety present in these polymers appears to be the most energetically favorable binding site for trinitrotoluene. Surface features of the polymer suggest that the small cavity feature of the pentiptycene moiety may be more available for binding to analyte compounds due to steric crowding about the large cavity. Binding energies between model binding sites of the polymer and various analyte compounds were more rigorously estimated by semiempirical and ab initio techniques. Binding energies were found to be largest with trinitrotoluene and other nitroaromatic compounds. Electrostatic and π-stacking interactions between trinitrotoluene and the model host were investigated by studying a series of modified host compounds.

1. Introduction

Fluorescence-based chemosensors have long been of interest for use in sensory materials due to their high degree of sensitivity [1,2]. Traditional fluorescent chemosensors measure the increase or decrease (quenching) in fluorescent intensity that results when a single analyte compound interacts with a single fluorophore. More recent developments in the field of fluorescence-based chemosensors have led to the development of a new class of materials termed amplifying fluorescent polymers (AFP), which consist of conjugated polymers possessing electronic properties that enhance the fluorescent response to analyte compounds [3–5]. AFP polymers generally consist of a conjugated polymer backbone containing a series of fluorophore and receptor groups. Absorption of light causes an excited electron to travel along the conjugated polymer backbone, interacting with many fluorophores and increasing the probability of a fluorescent event occurring. If a single electron-deficient analyte compound binds to the AFP chain a non-radiative energetic sink is formed that can potentially prevent emission from many fluorophores along the polymer chain. In this manner the quenching response in an AFP is greatly amplified in comparison to monomeric materials.

One application of AFP sensor materials has been in the area of explosive materials detection. Researchers at MIT have developed a polymer material, **1**, that has been shown to have a very large fluorescent quenching response to 2,4,6-trinitrotoluene (TNT) and 2,4-dinitrotoluene (DNT) [6–8]. This polymer consists of alternating pentiptycene and disubstituted benzene moieties, joined together by ethyne linker groups. The authors report that the incorporation of the rigid, non-planar pentiptycene moiety is key to this polymer's performance. The pentiptycene moiety is believed to cause the formation of cavities in the polymer structure that can incorporate small organic molecules, while larger molecules are excluded. The electron-rich aromatic rings of the pentiptycene receptor moiety form an electrostatic complement to electron-deficient, planar, nitroaromatic compounds. Finally, absorption and fluorescence spectra indicate that the pentiptycene moieties greatly reduce π-stacking or excimer formation between adjacent polymer backbones, which leads to greater fluorescent stability. Note that the pentiptycene moiety possesses two differing faces that could potentially serve as binding sites for small molecules: a "small cavity" consisting of three ring structures, and a "large cavity" consisting of five ring structures.

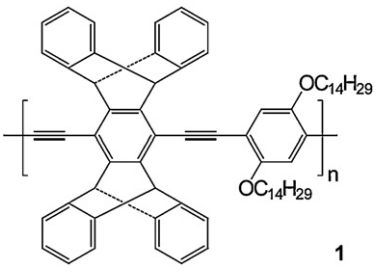

1

* Tel.: +1 850 767 0100; fax: +1 850 767 0101.
E-mail address: menlow@ara.com

1093-3263/$ – see front matter © 2011 Elsevier Inc. All rights reserved.
doi:10.1016/j.jmgm.2011.09.001

Polymer **1** was used in the development and commercialization of a sensor known as Fido by FLIR Systems Inc. (formally Nomadics Inc.) [9–12]. This sensor has been shown to be able to detect single-femtogram quantities of vapor-phase nitroaromatic compounds in real time. Although the AFP polymer **1** and the Fido system were originally developed for the detection of nitroaromatic compounds, the Fido sensor has also proven to be effective for the detection of a number of additional explosive compounds including cyclotrimethylenetrinitramine (RDX), and pentaerythritol tetranitrate (PETN) [13]. This is somewhat surprising given that these non-aromatic, relatively non-planar compounds might not be expected to bind strongly to the pentiptycene moieties present in polymer **1**.

The fluorescent quenching response of an AFP per unit time is proportional to the concentration (or vapor pressure) of the analyte compound (C), the free energy change associated with the transfer of an electron from the excited polymer to the analyte compound (ΔG^0), and the binding constant between the analyte and the polymer (K_b). This relationship may be expressed as

$$FQ \propto C\exp(-\Delta G^0)^2 K_b \quad (1)$$

Thus for efficient fluorescent quenching to occur at low concentrations the analyte compound and the polymer must have standard reduction and oxidation potentials of sufficient magnitude to result in a negative free energy change in the electron transfer process and the binding constant between the analyte and polymer must be large.

Although it is suspected that analyte compounds bind to the aromatic face of the pentiptycene moieties in polymer **1**, the binding geometries and interaction energies for this process have not been examined in detail to date. Understanding how TNT and other analyte compounds binding to polymer **1** can aid in understanding the excellent performance of this polymer system and provide insight to aid the development of next-generation polymers with enhanced fluorescent response to TNT or other analyte compounds of interest. This work uses molecular dynamics methods to examine the surface structural features present in films of polymer **1**, and to explore the interaction between this polymer system and analyte molecules. Semiempirical and ab initio methods are then used to more rigorously examine the binding geometries and binding energies between likely binding sites in the polymer and a number of analyte compounds. Finally, binding energies between TNT and several modified polymer binding sites are evaluated in order to estimate the effect that electrostatic interaction and π-stacking has upon binding energies.

2. Methods

Molecular dynamics simulations were carried out using the program NAMD [14]. The CHARMM force field version C35B2 was used, with additional parameters added to describe the ether and ethyne functional groups present in the model polymer [15–19]. All molecular dynamics simulations described below were conducted using step size of 1 μs per time step. Three-dimensional periodic boundary conditions were imposed upon the simulation space. Temperature rescaling was used to maintain the system at 300 K. Simulation setup, visualization and analysis were conducted using the programs PackMol and VMD [20,21].

Ab initio electronic structure calculations were carried out using the program GAMESS [22,23]. Geometry optimizations under full symmetry constraints were performed for the model host compounds and all analyte compounds at the RHF/6-31G(d,p) and B3LYP/6-31G(d,p) levels of theory [24–29]. Frequency calculations were performed to insure that local minima structures had been identified. Partial atomic charges were obtained by performing a Mulliken population analysis on the RHF/6-31G(d,p) wavefunction [30]. Electrostatic potential contour diagrams were generated from these data using the program Molekel [31].

Binding energies for several host and analyte combinations were calculated using the semiempirical free energy force field package Autodock, version 4.2 [32]. Input geometries for the host and analyte compounds were taken from either the molecular dynamics simulation results or from the ab initio optimized geometries, as described below. In all cases the host compound was constrained to be rigid while the analyte compound was permitted full torsional flexibility. Docking energies were calculated using partial atomic charges generated by the default Gasteiger method [33], and also using partial atomic charges obtained from the Mullikan population analysis at the RHF/6-31G(d,p) level of theory.

Binding energies for certain host-and-analyte pairs were also calculated at the ab initio level of theory by taking the difference in zero-point vibrational energy corrected total energies between the isolated species and the complex at both the RHF/6-31G(d,p) and B3LYP/6-31G(d,p) levels of theory. In those cases, full geometry optimizations were performed on the host analyte complex using the minimal-energy Autodock geometry as a starting point, followed by frequency calculations to ensure that a local minimum had been identified.

$$\text{BindingEnergy} = E(\text{complex}) - E(\text{host}) - E(\text{analyte}) \quad (2)$$

3. Results and discussion

The first step undertaken was to develop a model polymer structure to simulate the surface features present in an AFP polymer film. A model polymer segment, **2**, was constructed by joining four pentiptycene segments, four disubstitued benzene segments, and nine ethyne linker groups. Three of these polymer segments were randomly (subject to a 2-ångstrom distance tolerance) placed into a cubic simulation space 100 Å on a side. A 500-step energy minimization followed by a 500,000-time-step molecular dynamics simulation was then performed on the system, subject to the constraints given above. This procedure was repeated a total of ten times.

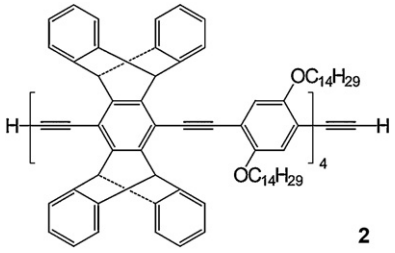

2

In all ten simulations the three model polymer segments coalesced into a single cluster. The polymer backbone of all segments remained approximately linear, with the backbones of the three polymer segments roughly parallel to each other. The two aliphatic side chain substituents of the benzene segments were observed to extend over the surface of the polymer cluster, partially obstructing the aromatic surfaces of neighboring pentiptycene moieties, including those on neighboring polymer chains. The smaller-cavity regions of the pentiptycene moieties, which extend further from the polymer axis, are seen to be less involved with the aliphatic side chains and, in general, protrude from the polymer cluster to a greater extent than do the larger-cavity regions of the pentiptycene moieties. This suggests that the small-cavity features of the pentiptycene moieties may be more available for binding with analyte compounds than the more-entangled and -obscured large-cavity features. No large cavities or pores of appropriate size to incorporate a small organic molecule such as TNT, as are suspected to exist in the macroscopic polymer structure, were observed. Is it likely

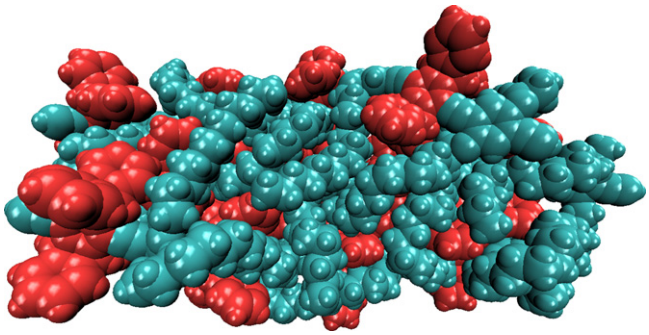

Fig. 1. Results of a molecular dynamics simulation consisting of three AFP polymer chains (blue) containing four pentiptycene segments (red) each. (For interpretation of the references to color in this figure legend, the reader is referred to the web version of the article.)

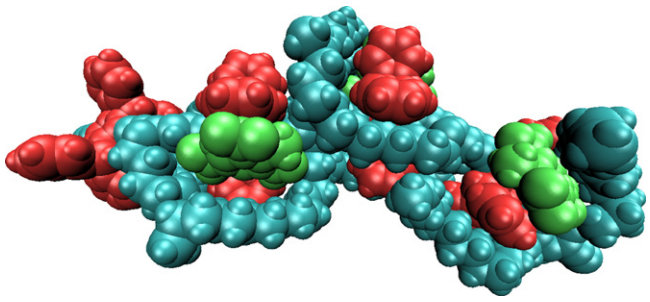

Fig. 2. Results of a molecular dynamics simulation consisting of three trinitrotoluene molecules (green) bound to pentiptycene binding sites (red) in an AFP chain (blue). Two trinitrotoluene molecules are sandwiched between a pentiptycene cavity and the polymer aliphatic side chains.

that this model polymer system is too small to form such features. A screenshot of a cluster of three model polymer chains at the end of a simulation is shown in Fig. 1.

The next step was to observe how TNT analyte molecules interact with the polymer clusters generated in the previous step. Three TNT molecules were added to the simulation space of each polymer cluster in random locations. A further 500,000-time-step molecular dynamics simulation was performed on each resulting system, subject to the same constraints given above.

During these simulations, the TNT molecules were observed to drift through space until they made contact with the polymer cluster. TNT molecules that contacted the large or small cavity of the pentiptycene segment remained at these sites, indicating that the TNT molecules have a strong energetic affinity for these sites. TNT molecules that made contact with the benzene segment or aliphatic side chains migrated over the surface of the polymer cluster, often until they reached the large or small cavity of a pentiptycene moiety. In no cases was a TNT molecule observed leaving a pentiptycene binding site and migrating to other features on the polymer. Similarly, no TNT molecules were observed to detach themselves from the polymer surface and return to the surrounding space. Of the thirty total TNT molecules present in the ten simulations performed, six remained drifting in space without having made contact with the polymer cluster, five ended the simulation bound to the large cavity of a pentiptycene moiety, twelve ended the simulation bound to the small cavity of a pentiptycene moiety, and seven ended the simulation located on other regions of the polymer surface.

Of particular interest was the tendency of a TNT molecule to become sandwiched between one face of a pentiptycene moiety and the aliphatic side chain from a nearby benzene moiety located on the same or a neighboring polymer chain. This sandwiching likely increases the binding energy of the TNT molecule for this location and hinders it from migrating out of the binding site. A screenshot from a simulation illustrating this interaction is shown in Fig. 2.

After the series of molecular dynamics simulations indicated that the pentiptycene segment appeared to be the primary binding location for TNT in the model polymer segments, the next step was to estimate the binding energy between the pentiptycene segment and several small compounds relevant to explosives detection, including TNT. The pentiptycene diacetylene compound, **3**, was chosen to serve as a model for the pentiptycene binding site in the AFP polymer.

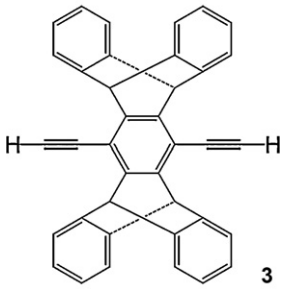

3

Binding energies between TNT and the large- and small-cavity binding sites of host compound **3** were calculated using Autodock and via ab initio methods. The results are shown in Table 1. Binding energies for the large cavity were largest at every level of theory except in the case of RHF/6-31G(d,p); there the energies were close to equivalent. The greatest difference in energy between the large and small cavities was obtained using the semiempirical Autodock method with Gasteiger partial atomic charges. Binding energies obtained via ab initio methods were significantly higher overall than with the semiempirical methods.

Minimal-energy binding geometries between TNT and the large- and small-cavity binding sites of host compound **3** are presented in Figs. 3 and 4. Geometries obtained using Autodock with Gasteiger partial atomic charges and obtained via RHF/6-31G(d,p) energy minimizations are shown. Geometries obtained using Autodock with ab initio partial atomic charges, and via B3LYP/6-31G(d,p) energy minimizations are virtually identical to predictions from the former methods, respectively.

In the case of binding at the large pentiptycene cavity (Fig. 3), somewhat different geometries are obtained at the differing levels of theory. The semiempirical Autodock methods results in the TNT positioned such that its aromatic ring is approximately parallel to one face of the large cavity and with two nitro groups oriented toward the center of the cavity. Ab intio methods result in the TNT molecule more symmetrically oriented with respect to the faces of

Table 1
Binding energies (kcal/mol) for host compound **2** and trinitrotoluene at several levels of theory.

Binding site	Autodock using Gasteiger charges	Autodock using RHF/6-31G(d,p) charges[a]	RHF/6-31G(d,p)[b]	B3LYP/6-31G(d,p)[b]
Large cavity	−2.95	−1.87	−5.19	−5.07
Small cavity	−1.79	−1.45	−5.31	−4.70

[a] Partial atomic charges for this data set were obtained through RHF/6-31G(d,p) calculations on isolated host and TNT compounds.
[b] RHF and B3LYP ab initio results include zero-point correction energies.

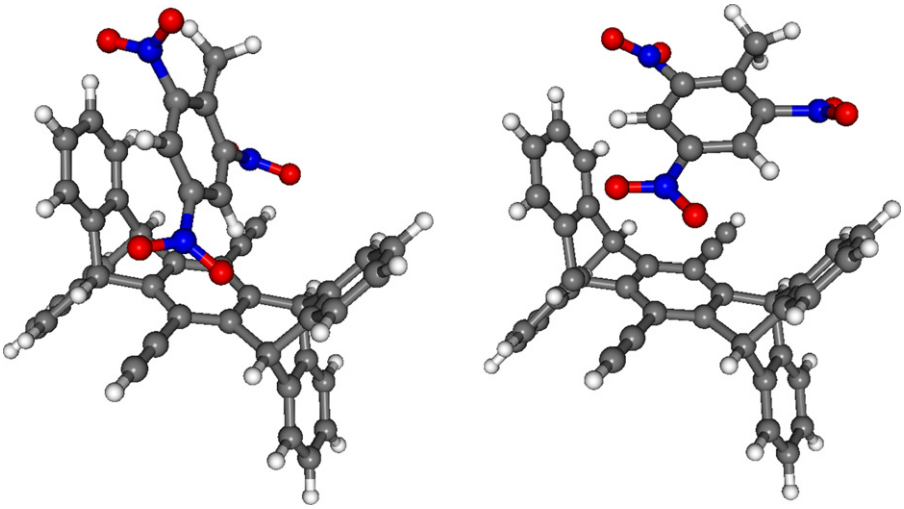

Fig. 3. Optimized geometries of a TNT molecule bound to the large cavity of host compound **3**, obtained via Autodock (left) and RHF/6-31G(d,p) (right) methods.

the large cavity and with one nitro group pointed into the interior of the large cavity. Very similar trends are observed for the case of binding at the small pentiptycene cavity (Fig. 4).

Binding energies between several additional analyte compounds relevant to explosives detection were also calculated using the semiempirical Autodock method and are presented in Table 2. Binding energies for nitrobenzene and DNT are very similar in magnitude to the binding energies seen with TNT. Binding energies for benzene are somewhat less than the energies seen with the nitrobenzene series. This is to be expected as the aromatic faces of the pentiptycene moiety are not electrostatically complementary with unsubstituted benzene as they are with the nitro-substituted benzene series. Binding energies for the remaining nonaromatic, generally nonplanar compounds are generally lower than those seen for the nitroaromatic series. Calculated binding energies for HMTD, NG, RDX, and TATP were all less than the binding energies obtained for TNT, in both the large and small pentiptycene cavities. Binding energies calculated for RDX in the small pentiptycene cavity and for NG in the large pentiptycene cavity are particularly small, being close to zero.

One particular trend observed is that analyte compounds bound to the large or small cavity often tended to orient themselves so that one or more nitro groups were oriented toward the center of the cavity. For instance, DMDNB bound to the pentiptycene large cavity adopted a geometry with its nitro groups nearly eclipsed (having a nearly zero N–C–C–N dihedral angle) and both nitro groups oriented toward the central six-membered backbone ring. However, DMDNB has been shown [34] to produce a low fluorescence-quenching response with polymer **1**. It may be the case that electron transfer between the pentiptycene moiety and a bound DMDNB is very inefficient, resulting in a low fluorescence-quenching response. Similarly, NG binding to the pentiptycene small cavity orients itself such that one nitro group is oriented toward the intersection of the two faces of the small cavity, with

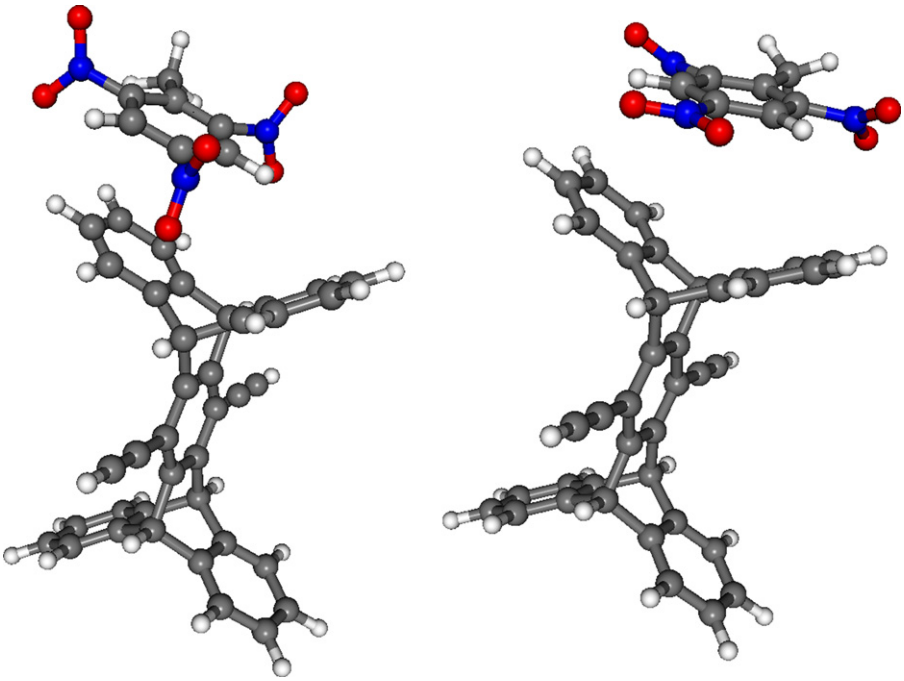

Fig. 4. Optimized geometries of a TNT molecule bound to the small cavity of host compound **3**, obtained via Autodock (left) and RHF/6-31G(d,p) (right) methods.

Table 2
Binding energies (kcal/mol) for host compound **3** and several analyte compounds.

Analyte	Binding site	Autodock using Gasteiger charges	Autodock using RHF/6-31G(d,p) charges[a]
Trinitrotoluene (TNT)	Large cavity	−2.95	−1.87
	Small cavity	−1.79	−1.45
2,4-Dinitrotoluene (DNT)	Large cavity	−3.02	−1.88
	Small cavity	−1.88	−1.15
Nitrobenzene	Large cavity	−2.92	−1.96
	Small cavity	−1.78	−1.18
Benzene	Large cavity	−2.42	−1.66
	Small cavity	−1.55	−1.04
Dimethyldinitrobutane (DMDNB)	Large cavity	−3.39	−2.29
	Small cavity	−2.05	−0.64
Hexamethylene triperoxide diamine (HMTD)	Large cavity	−3.54	−1.64
	Small cavity	−1.85	−0.81
Nitroglycerin (NG)	Large cavity	−4.08	−0.03
	Small cavity	−2.47	−0.65
Cyclotrimethylenetrinitramine (RDX)	Large cavity	−4.23	−0.56
	Small cavity	−2.69	−0.07
Triacetone triperoxide (TATP)	Large cavity	−3.18	−1.84
	Small cavity	−2.04	−1.18

[a] Partial atomic charges for this data set were obtained through RHF/6-31G(d,p) calculations on isolated host and analyte compounds.

the majority of the molecule—including the two remaining nitro groups—extending out of the cavity and having no contact with the cavity surface. The low binding energy of NG at this binding site may be a result of this limited contact between the two species.

The next area investigated was the effect that modifying model host **3** with certain substituents has upon its binding energy with TNT. The pentiptycene moiety has been frequently described as being the electrostatic complement of electron-deficient molecules such as TNT [6–8]. Complimentary electrostatics leads to enhanced binding energy due to more energetically favorable π-stacking interactions between the faces of the pentiptycene and the aromatic ring of the analyte compound. Fig. 5 displays electrostatic potential contour diagrams for pentiptycene and for TNT. It should be possible to modify this effect by replacing the pentiptycene hydrogen atoms with electron-donating or -accepting functional groups. This strategy has been successfully employed to modify the π-stacking interactions in diarylnaphthalenes [35]. Model host **4**, in which 16 hydrogen atoms were replaced with fluorine atoms, and model host **5**, in which eight hydrogen atoms were replaced with eight methoxy groups, were used to study this effect.

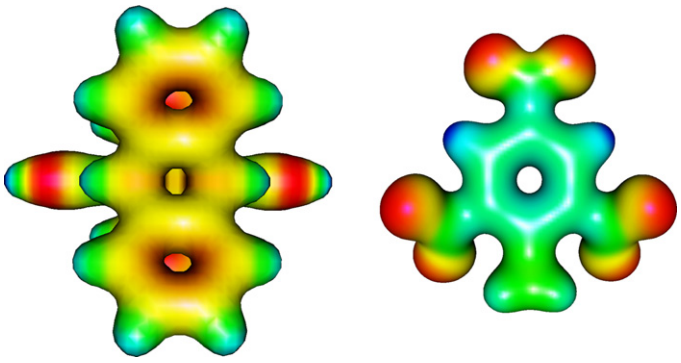

Fig. 5. Electrostatic potential contour for host compound **3** (left, showing the small cavity face) and for a trinitrotoluene molecule (right).

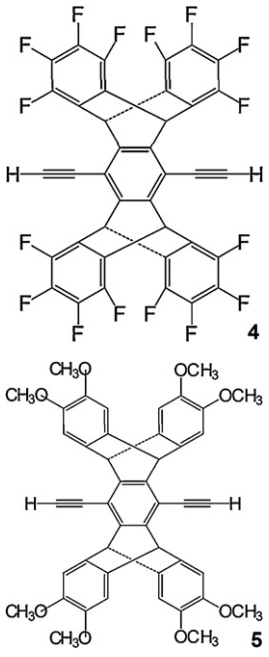

Table 3
Binding energies (kcal/mol) for TNT and host compounds **3** through **7**.

Host	Binding site	Autodock using Gasteiger charges	Autodock using RHF/6-31G(d,p) charges[a]
3	Large cavity	−2.95	−1.87
	Small cavity	−1.79	−1.45
4	Large cavity	−3.24	−1.89
	Small cavity	−1.95	−0.10
5	Large cavity	−3.69	−1.74
	Small cavity	−2.84	−1.22
6	Large cavity	−3.53	−2.20
	Small cavity	−2.65	−1.75
7	Large cavity	−4.49	−2.97
	Small cavity	−3.58	−2.54

[a] Partial atomic charges for this data set were obtained through RHF/6-31G(d,p) calculations on isolated host and TNT compounds.

Binding energies between TNT and hosts **4** and **5** were calculated using Autodock under the same methodology described above. The results of the calculations are presented in Table 3. Host **4**, which incorporated electron withdrawing groups, is expected to have reduced binding energies due to reduced complementary π-stacking interaction with TNT. Indeed, the binding energy at the small cavity of host **4** is reduced almost to zero. Interestingly, the large cavity's binding energy is essentially unchanged. Host **5**, which incorporated electron-donating groups, is expected to have enhanced binding energies. However, calculations reveal that the binding energies are almost unchanged, and are in fact slightly lower than for the unsubstituted host **3**. Examination of the geometry that the TNT adopts when bound to host **5** shows that—especially in the case of binding in the small cavity of host **5**—the nitro groups in the TNT molecule are brought in close proximity to the methoxy groups in the host compound. It appears that any beneficial π-stacking interaction brought about by the electron-donating methoxy groups is essentially offset by the negative interaction between the electron-rich nitro groups on the TNT molecule and the electron-rich methoxy groups on the host compound.

The final area investigated was the effect that increasing the size of the aromatic surfaces in the pentiptycene moiety had upon binding energies. Model hosts **6** and **7** were chosen, in which the eight terminal benzene structures were replaced with naphthalene and phenanthrene groups, respectively. These two structures provide increased aromatic surface area to potentially enhance the π-stacking interactions with TNT.

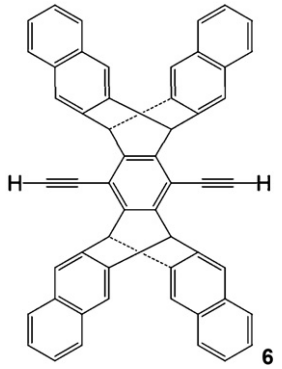

6

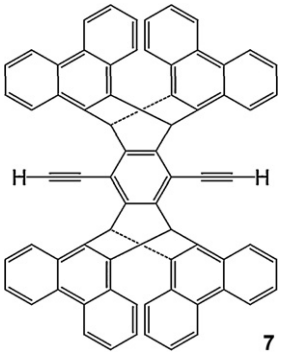

7

Binding energies between TNT and hosts **5** and **6** were calculated using Autodock under the same methodology described above. The results of the calculations are presented in Table 3. The naphthalene and phenanthrene analog hosts are seen to have progressively larger binding energies with increased aromatic surface area. Examination of the geometry that the bound TNT molecule adopts when bound to either cavity of hosts **6** and **7** reveal that the TNT molecule becomes localized on one face of the cavity, with the plane of the TNT molecule approximately parallel with one face of the host, in contrast to binding in host **3,** where the TNT was observed to be more symmetrically located within the cavity. The increased π-stacking interactions seen with hosts **6** and **7** contribute to their larger binding energies and may result in greater electron transfer efficiency.

4. Conclusion

The molecular dynamics simulations carried out in this work suggest several avenues for future research. Expanded molecular dynamics simulations of larger polymer clusters can be performed to investigate the macroscopic pores that are suspected to form in AFP polymer systems. Simulations of the interaction of non-planar, nonaromatic compounds such as NG with the AFP polymer may reveal that regions other than the pentiptycene moieties play a role in binding in these types of compounds. A more systematic investigation on the effect that substitution and modification of the pentiptycene binding sites has upon binding energies may lead to polymer moieties with enhanced binding and fluorescent quenching response for TNT or other analyte compounds of interest.

Disclaimer

This material is based upon work supported by the Air Force Research Laboratory (AFRL) under contract no. FA4819-09-C-0027. Reference herein to any specific commercial product, process, or service by trade name, trademark, manufacturer, or otherwise does not constitute or imply its endorsement, recommendation, or approval by the United States Air Force. The views and opinions of authors expressed herein do not necessarily state or reflect those of the United States Air Force. Any opinions, findings, and conclusions or recommendations expressed in this material are those of the author(s) and do not reflect the views of AFRL.

This report was prepared as an account of work sponsored by the United States Air Force. Neither the United States Air Force, nor any of its employees, makes any warranty, expressed or implied, or assumes any legal liability or responsibility for the accuracy, completeness, or usefulness of any information, apparatus, product, or process disclosed, or represents that its use would not infringe privately owned rights.

References

[1] Fluorescent chemosensors for ion and molecular recognition, in: A.W. Czarnik (Ed.), ACS Symposium Series 538, American Chemical Society, Washington DC, 1993.
[2] J.P. Desvergne, A.W. Czarnik (Eds.), Chemosensors of Ion and Molecule Recognition, Kluwer Academic Publishers, Boston, 1997.
[3] Q. Zhou, T.M. Swager, J. Am. Chem. Soc. 117 (1995) 7017.
[4] Q. Zhou, T.M. Swager, J. Am. Chem. Soc. 117 (1995) 12593.
[5] S.W. Thomas, G.D. Joly, T.M. Swager, Chem. Rev. 107 (2007) 1339–1386.
[6] J.S. Yang, T.M. Swager, J. Am. Chem. Soc. 120 (1998) 5321–5322.
[7] J.S. Yang, T.M. Swager, J. Am. Chem. Soc. 120 (1998) 11864–11873.
[8] Detection of explosives using amplified fluorescent polymers, in: M. Marshall, J.C. Oxley (Eds.), Aspects of Explosives Detection, Elsevier B.V., 2009.
[9] M. laGrone, C. Cumming, M. Fisher, D. Reust, et al., Landmine detection by chemical signature: detection of vapors of nitroaromatic compounds by fluorescence quenching of novel polymer materials, in: Proceedings of SPIE, Detection and Remediation Technologies for Mines and Minelike Targets IV, vol. 3710, part 1, 1999, pp. 409–420.
[10] M. laGrone, C. Cumming, M. Fisher, M. Fox, S. Jacob, D. Reust, M. Rockley, E. Towers, Detection of landmines by amplified fluorescence quenching of polymer films: a man portable chemical sniffer for detection of ultratrace concentrations of explosives emanating from landmines, in: Proceedings of SPIE, Detection and Remediation Technologies for Mines and Minelike Targets V, vol. 4038, part 1, 2000, pp. 553–562.
[11] C. Cumming, C. Aker, M. Fisher, M. Fox, M. laGrone, D. Reust, M. Rockley, T. Swager, E. Towers, V. Williams, Using novel fluorescent polymers as sensory materials for above-ground sensing of chemical signature compounds emanating from buried landmines, IEEE Trans. Geosci. Remote Sensing 39 (6) (2001) 1119–1128.
[12] M.E. Fischer, M. la Grone, J. Sikes, Implementation of serial amplifying fluorescent polymer arrays for enhanced chemical vapor sensing of landmines, Proc. SPIE 5089 (2003) 991.

[13] Fido Explosives Detectors Technical Overview, ICx Technologies.
[14] J.C. Phillips, R. Braun, W. Wang, J. Gumbart, E. Tajkhorshid, E. Villa, C. Chipot, R.D. Skeel, L. Kale, K. Schulten, Scalable molecular dynamics with NAMD, J. Comput. Chem. 26 (2005) 1781–1802.
[15] B.R. Brooks, R.E. Bruccoleri, B.D. Olafson, D.J. States, S. Swaminathan, M. Karplus, CHARMM: a program for macromolecular energy, minimization, and dynamics calculations, J. Comput. Chem. 4 (1983) 187–217.
[16] A.D. MacKerell Jr., B. Brooks, C.L. Brooks III, L. Nilsson, B. Roux, Y. Won, M. Karplus, in: P. v. R. Schleyer, et al. (Eds.), CHARMM: The Energy Function and its Parameterization With an Overview of the Program, The Encyclopedia of Computational Chemistry, vol. 1, John Wiley & Sons, Chichester, 1998, pp. 271–277.
[17] I. Vorobyov, V.M. Anisimov, S. Greene, R.M. Venable, A. Moser, R.W. Pastor, A.D. MacKerell Jr., Additive and classical drude polarizable force fields for linear and cyclic ethers, J. Chem. Theor. Comput. 3 (2007) 1120–1133.
[18] H. Lee, R.M. Venable, A.D. MacKerell Jr., R.W. Pastor, Molecular dynamics studies of polyethylene oxide and polyethylene glycol: hydrodynamic radius and shape anisotropy, Biophys. J. 95 (2008) 1590–1599.
[19] Parameters for the ethyne functional group were developed in-house based upon ab initio RHF/6-31G(d,p) calculations on the compound phenylacetylene (C6H5–CCH). These crude parameters were deemed adequate as the ethyne groups in the AFP and model compounds do not appear to play a significant role in binding with analyte compounds.
[20] W. Humphrey, A. Dalke, K. Schulten, VMD - visual molecular dynamics, J. Mol. Graph. 14 (1996) 33–38.
[21] L. Martínez, R. Andrade, E.G. Birgin, J.M. Martínez, Packmol: a package for building initial configurations for molecular dynamics simulations, J. Comput. Chem. 30 (13.) (2009) 2157–2164.
[22] M.W. Schmidt, K.K. Baldridge, J.A. Boatz, S.T. Elbert, M.S. Gordon, J.H. Jensen, S. Koseki, N. Matsunaga, K.A. Nguyen, S.J. Su, T.L. Windus, M. Dupuis, J.A. Montgomery, General atomic and molecular electronic structure system, J. Comput. Chem. 14 (1993) 1347–1363.
[23] M.S. Gordon, M.W. Schmidt, Advances in electronic structure theory: GAMESS a decade later, in: C.E. Dykstra, G. Frenking, K.S. Kim, G.E. Scuseria (Eds.), Theory and Applications of Computational Chemistry, the First Forty Years, Elsevier, Amsterdam, 2005, pp. 1167–1189, Chapter 41.
[24] C.C.J. Roothaan, Rev. Mod. Phys. 23 (1951) 69–89.
[25] A.D. Becke, J. Chem. Phys. 98 (1993) 1372–1377.
[26] P.J. Stephens, F.J. Devlin, C.F. Chablowski, M.J. Frisch, J. Phys. Chem. 98 (1994) 11623–11627.
[27] R.H. Hertwig, W. Koch, Chem. Phys. Lett. 268 (1997) 345–351.
[28] W.J. Hehre, R.F. Stewart, J.A. Pople, J. Chem. Phys. 51 (1969) 2657–2664.
[29] W.J. Hehre, R. Ditchfield, R.F. Stewart, J.A. Pople, J. Chem. Phys. 52 (1970) 2769–2773.
[30] R.S. Mulliken, J. Chem. Phys. 23 (1955) (1833–1840, 1841–1846, 2338–2342, 2343–2346).
[31] U. Varetto, MOLEKEL Version 4.3; Swiss National Supercomputing Centre: Manno (Switzerland).
[32] G.M. Morris, R. Huey, W. Lindstrom, M.F. Sanner, R.K. Belew, D.S. Goodsell, A.J. Olson, Autodock4 and AutoDockTools4: automated docking with selective receptor flexibility, J. Comput. Chem. 30 (2009) 2785–2791.
[33] J. Gasteiger, M. Marsili, A new model for calculating atomic charges in molecules, Tetrahedron Lett. 34 (1978) 3181–3184.
[34] S.W. Thomas, J.P. Amara, R.E. Bjork, T.M. Swager, Chem. Commun. (2005) 4572–4574.
[35] F. Cozzi, R.A. Ponzini, M. Cinquini, J. Siegel, Angew. Chem. Int. Ed. Engl. 34 (1995) 9.